

# Photoluminescence properties of *in situ* Tm-doped $\text{Al}_x\text{Ga}_{1-x}\text{N}$

U. Hömmerich<sup>a)</sup> and Ei Ei Nyein

Department of Physics, Hampton University, Hampton, Virginia 23668

D. S. Lee and A. J. Steckl

University of Cincinnati, Nanoelectronics Laboratory, Cincinnati, Ohio 45221

J. M. Zavada

US Army Research Office, Durham, North Carolina 27709

(Received 8 August 2003; accepted 10 October 2003)

We report on the photoluminescence (PL) properties of *in situ* Tm-doped  $\text{Al}_x\text{Ga}_{1-x}\text{N}$  films ( $0 \leq x \leq 1$ ) grown by solid-source molecular-beam epitaxy. It was found that the blue PL properties of  $\text{Al}_x\text{Ga}_{1-x}\text{N}:\text{Tm}$  greatly change as a function of Al content. Under above-gap pumping, GaN:Tm exhibited a weak blue emission at  $\sim 478$  nm from the  $^1\text{G}_4 \rightarrow ^3\text{H}_6$  transition of  $\text{Tm}^{3+}$ . Upon increasing Al content, an enhancement of the blue PL at 478 nm was observed. In addition, an intense blue PL line appeared at  $\sim 465$  nm, which is assigned to the  $^1\text{D}_2 \rightarrow ^3\text{F}_4$  transition of  $\text{Tm}^{3+}$ . The overall blue PL intensity reached a maximum for  $x=0.62$ , with the 465 nm line dominating the visible PL spectrum. Under below-gap pumping, AlN:Tm also exhibited intense blue PL at 465 and 478 nm, as well as several other PL lines ranging from the ultraviolet to near-infrared. The  $\text{Tm}^{3+}$  PL from AlN:Tm was most likely excited through defect-related complexes in the AlN host.

© 2003 American Institute of Physics. [DOI: 10.1063/1.1631742]

Light emission from rare-earth (RE)-doped III-N semiconductors is of significant current interest for applications in electroluminescence (EL) devices.<sup>1–4</sup> Previous work on visible emission from RE-doped III-Ns was mainly focused on RE-doped GaN.<sup>1–3</sup> Photoluminescence (PL) and cathodoluminescence (CL) data have been reported from nearly all lanthanide ions doped into GaN.<sup>1–3</sup> Visible EL devices based on RE-doped GaN, however, have only been demonstrated from GaN:Eu (red),<sup>1,5,6</sup> GaN:Er (green),<sup>7</sup> and GaN:Tm (blue).<sup>8</sup> One of the main challenges in using RE-doped GaN for full-color display applications is obtaining efficient blue emission. While dominant blue emission has been reported from GaN:Tm EL devices,<sup>8,9</sup> the overall device efficiency was significantly lower than results obtained for GaN:Eu (red) and GaN:Er (green).<sup>2</sup> For RE-doped AlN, red emission has also been reported from Eu, and green emission from Er- and Tb-doped amorphous and crystalline films.<sup>10–12</sup> Recently, blue CL was reported from Tm-impanted AlN<sup>13</sup> and efficient blue EL was demonstrated from *in situ* Tm-doped AlGaIn films.<sup>14</sup>

In this letter, we report on the PL properties of  $\text{Al}_x\text{Ga}_{1-x}\text{N}:\text{Tm}$  films under above- and below-gap pumping. Tm-doped  $\text{Al}_x\text{Ga}_{1-x}\text{N}$  films with  $x=0$  (GaN), 0.16, 0.29, 0.39, 0.62, 0.81, and 1 (AlN) were grown by solid-source molecular-beam epitaxy on *p*-type Si (111) substrates. Elemental Al, Ga, and RE sources were used in conjunction with a rf-plasma source supplying atomic nitrogen. The Tm cell temperature was fixed at 600 °C, leading to a Tm concentration between  $\sim 0.2$  and  $\sim 0.5$  at. %. The  $\text{Al}_x\text{Ga}_{1-x}\text{N}:\text{Tm}$  films were grown for 1 h at 550 °C and a growth rate of  $\sim 0.5$   $\mu\text{m}/\text{h}$ . Adjusting the Al cell temperature during growth controlled the Al content in the films. The

total flux of Ga and Al was kept constant. The PL was excited using the UV output (250 nm, 10 ns pulses, 10 Hz repetition rate) of an optical parametric oscillator (OPO) system. For low-temperature PL measurements, the samples were mounted on the cold finger of a closed-cycle helium refrigerator. Visible PL spectra were recorded using a 0.5 m monochromator equipped with a photomultiplier tube for light detection. The signal was processed using a boxcar averager, and PL lifetime transients were recorded using a digitizing oscilloscope.

Figure 1 shows an overview of the normalized PL spectra of Tm-doped  $\text{Al}_x\text{Ga}_{1-x}\text{N}$  with  $x=0, 0.16, 0.21, 0.39, 0.62$ , and  $0.81$ . The calculated bandgap energies using Vegard's law and a bowing parameter of  $b=1$  are 3.39 eV (GaN), 3.71, 3.82, 4.26, 4.91, and 5.56 eV, respectively.<sup>15</sup> The PL was excited using the 250 nm ( $\sim 4.96$  eV) output of an OPO system, which corresponds to above-gap pumping for  $\text{Al}_x\text{Ga}_{1-x}\text{N}$  samples with  $x \leq 0.62$ . Similar to previous reports,<sup>8,9</sup> the visible PL from GaN:Tm is characterized by a broad band extending from  $\sim 400$  to 600 nm and near-band-edge emission at  $\sim 367$  nm. A weak blue PL line located at  $\sim 478$  nm from the  $^1\text{G}_4 \rightarrow ^3\text{H}_6$  transition of  $\text{Tm}^{3+}$  is hardly observable. The infrared PL at  $\sim 803$  nm is tentatively assigned to the intra- $4f$  transition  $^3\text{H}_4 \rightarrow ^3\text{H}_6$  of  $\text{Tm}^{3+}$  ions.<sup>9</sup> Changing from GaN:Tm to  $\text{Al}_x\text{Ga}_{1-x}\text{N}:\text{Tm}$  led to pronounced changes in the PL properties. Upon increasing Al content, the 478 nm PL line gained in intensity and was clearly observed. The broadband emission was also sharply reduced. The strongest emission from the  $^1\text{G}_4 \rightarrow ^3\text{H}_6$  transition at 478 nm was obtained for  $x=0.39$ . Interestingly, two other PL lines were observed: a weaker line at  $\sim 370$  nm and a dominant blue line at  $\sim 465$  nm. The PL intensity of the 465 nm line was several times larger compared to the 478 nm PL. The overall strongest blue PL intensity was measured

<sup>a)</sup>Electronic mail: uwe.hommerich@hamptonu.edu

Report Documentation Page				Form Approved OMB No. 0704-0188	
Public reporting burden for the collection of information is estimated to average 1 hour per response, including the time for reviewing instructions, searching existing data sources, gathering and maintaining the data needed, and completing and reviewing the collection of information. Send comments regarding this burden estimate or any other aspect of this collection of information, including suggestions for reducing this burden, to Washington Headquarters Services, Directorate for Information Operations and Reports, 1215 Jefferson Davis Highway, Suite 1204, Arlington VA 22202-4302. Respondents should be aware that notwithstanding any other provision of law, no person shall be subject to a penalty for failing to comply with a collection of information if it does not display a currently valid OMB control number.					
1. REPORT DATE <b>OCT 2003</b>		2. REPORT TYPE		3. DATES COVERED <b>00-00-2003 to 00-00-2003</b>	
4. TITLE AND SUBTITLE <b>Photoluminescence properties of in situ Tm-doped AlxGa1-xN</b>				5a. CONTRACT NUMBER	
				5b. GRANT NUMBER	
				5c. PROGRAM ELEMENT NUMBER	
6. AUTHOR(S)				5d. PROJECT NUMBER	
				5e. TASK NUMBER	
				5f. WORK UNIT NUMBER	
7. PERFORMING ORGANIZATION NAME(S) AND ADDRESS(ES) <b>University of Cincinnati,Nanoelectronics Laboratory,Cincinnati,OH,45221-0030</b>				8. PERFORMING ORGANIZATION REPORT NUMBER	
9. SPONSORING/MONITORING AGENCY NAME(S) AND ADDRESS(ES)				10. SPONSOR/MONITOR'S ACRONYM(S)	
				11. SPONSOR/MONITOR'S REPORT NUMBER(S)	
12. DISTRIBUTION/AVAILABILITY STATEMENT <b>Approved for public release; distribution unlimited</b>					
13. SUPPLEMENTARY NOTES					
14. ABSTRACT					
15. SUBJECT TERMS					
16. SECURITY CLASSIFICATION OF:			17. LIMITATION OF ABSTRACT	18. NUMBER OF PAGES <b>3</b>	19a. NAME OF RESPONSIBLE PERSON
a. REPORT <b>unclassified</b>	b. ABSTRACT <b>unclassified</b>	c. THIS PAGE <b>unclassified</b>			

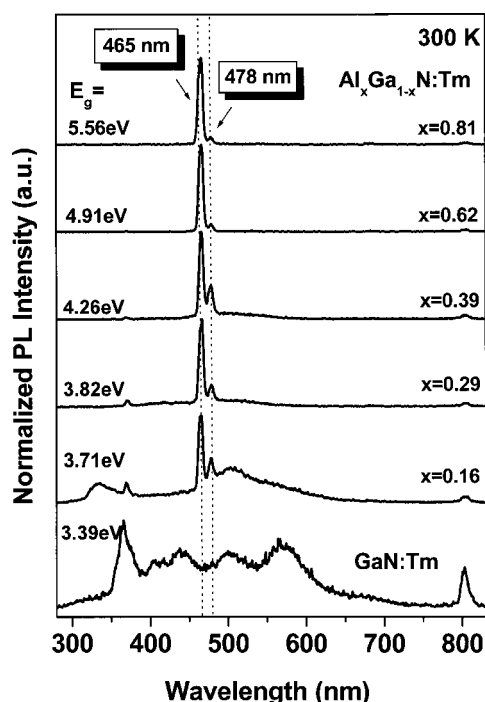


FIG. 1. Room-temperature PL spectra of  $\text{Al}_x\text{Ga}_{1-x}\text{N:Tm}$  excited at 250 nm. The dotted lines indicate the position of the blue PL arising from the transitions  $^1\text{G}_4 \rightarrow ^3\text{H}_6$  ( $\sim 478$  nm) and  $^1\text{D}_2 \rightarrow ^3\text{F}_4$  ( $\sim 465$  nm). The calculated bandgap energies ( $E_g$ ) are also indicated in the figure.

from  $\text{Al}_{0.62}\text{Ga}_{0.38}\text{N:Tm}$  with the 465 nm line being roughly ten times more intense than the 478 nm line.

The observation of new PL lines in  $\text{Al}_x\text{Ga}_{1-x}\text{N:Tm}$  can be explained by the change in bandgap energy of the host.  $\text{Tm}^{3+}$  has higher excited states above the  $^1\text{G}_4$  level, which are located at  $\sim 3.4$  eV ( $^1\text{D}_2$ ) and  $\sim 4.2$  eV ( $^1\text{I}_6/{}^3\text{P}_0$ ).<sup>16,17</sup> The energy of the  $^1\text{D}_2$  level is very similar to the bandgap energy of GaN (see Fig. 3). Therefore, no emission from the  $^1\text{D}_2$  level is observed from GaN:Tm. Upon increasing the bandgap energy of  $\text{Al}_x\text{Ga}_{1-x}\text{N}$ , the  $\text{D}_2$  level moves within the bandgap of the host, which results in the observation of PL lines at 370 and 465 nm. Based on the comparison to existing literature,<sup>16,17</sup> the 370 and 465 nm lines are assigned to the  $^1\text{D}_2 \rightarrow ^3\text{H}_6$  and  $^1\text{D}_2 \rightarrow ^3\text{F}_4$  transitions of  $\text{Tm}^{3+}$ .

Figure 1 also indicates that the excitation efficiency of the  $^1\text{G}_4$  level of  $\text{Tm}^{3+}$  is enhanced in  $\text{Al}_x\text{Ga}_{1-x}\text{N:Tm}$  samples compared to GaN:Tm. As mentioned earlier, hardly any blue  $\text{Tm}^{3+}$  PL was observed in GaN:Tm. A similar poor above-gap pumping efficiency was reported for  $\text{Tb}^{3+}$  ions in GaN:Tb.<sup>18</sup> The weak PL excitation efficiency was explained using a defect-related energy transfer model as proposed by Takahei *et al.* for RE-doped semiconductors.<sup>19</sup> In this model, RE doping of a semiconductor leads to the formation of RE-related levels in the bandgap of the host. These levels can trap free carriers, which subsequently recombine and transfer their energy to intra-4f RE transitions. Recent studies have identified RE-related traps for GaN:Eu,<sup>19,20</sup> GaN:Tb,<sup>19</sup> and GaN:Er<sup>21</sup> at  $\sim 0.3$ – $0.4$  eV below the conduction band of GaN. The recombination energy of carriers trapped at the RE-related defects in GaN is then estimated to be  $\sim 3.0$ – $3.1$  eV, which energetically matches intra-4f transitions of  $\text{Eu}^{3+}$  and  $\text{Er}^{3+}$ , respectively.<sup>16</sup> On the other hand,  $\text{Tb}^{3+}$  ions do not exhibit intra-4f transitions in that energy range, prevent-

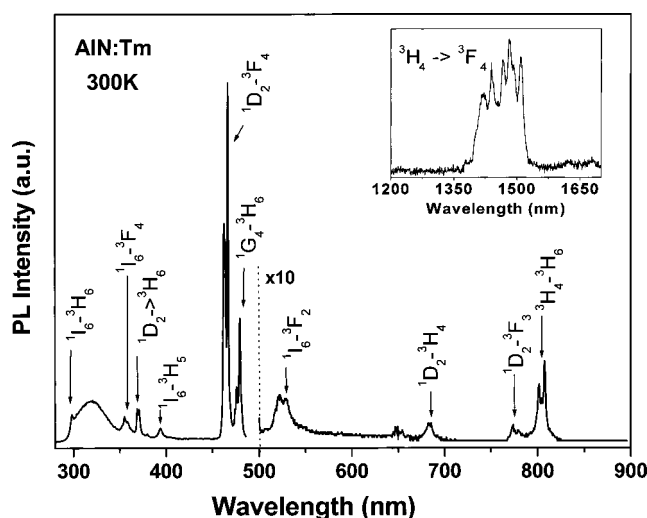


FIG. 2. High-resolution PL spectrum of AlN:Tm at room temperature. The PL was excited at 250 nm, which correspond to below-gap pumping. The assignment of the intra-4f transitions of  $\text{Tm}^{3+}$  is indicated in the figure. The inset shows the infrared PL spectrum around 1450 nm.

ing an efficient carrier-mediated excitation process in GaN:Tb. Assuming that  $\text{Tm}^{3+}$  also induces a defect-level in GaN, similar arguments for the weak above-gap excitation efficiency can be applied to GaN:Tm. Within the defect-related energy transfer model, however, the excitation efficiency of the  $\text{Tm}^{3+}$  can be optimized by a modification of the bandgap energy. Upon increasing Al content, higher excited states of  $\text{Tm}^{3+}$  ( $^1\text{D}_2/{}^1\text{I}_6/{}^3\text{P}_1$ ) move within the bandgap of  $\text{Al}_x\text{Ga}_{1-x}\text{N}$ , which provide additional channels for the energy transfer between defect levels and  $\text{Tm}^{3+}$  ions. Future investigations are necessary to identify Tm-related defects in  $\text{Al}_x\text{Ga}_{1-x}\text{N:Tm}$  to support the defect-related energy transfer model. In addition, it cannot be excluded that chemical effects related to the presence of Al change the  $\text{Tm}^{3+}$  incorporation and excitation mechanisms, similar to observations made for Er-doped AlGaAs.<sup>22</sup>

The high-resolution PL spectrum, with excitation at 250 nm, of AlN:Tm at room temperature is shown in Fig. 2. The PL was dominated by intense blue PL lines centered at  $\sim 465$  and  $\sim 478$  nm. The average lifetimes of the 465 and 478 nm lines were determined to be  $\sim 2$  and  $\sim 33$   $\mu\text{s}$ , respectively. The lifetimes were nearly temperature independent, suggesting that nonradiative decay processes are small. The different

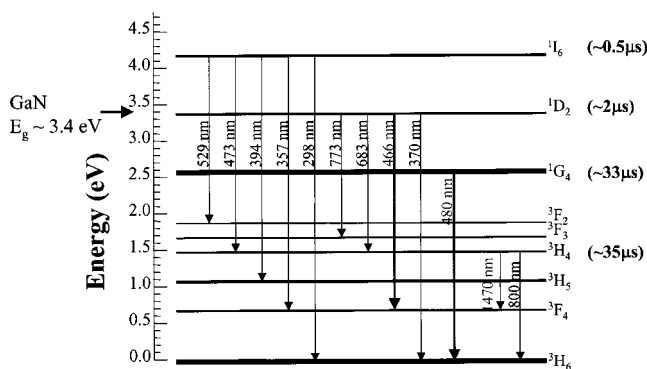


FIG. 3. Free-ion energy level diagram of  $\text{Tm}^{3+}$  ions and observed transitions in AlN:Tm. The bandgap of GaN is also indicated in the figure, along with PL lifetimes for several excited states of  $\text{Tm}^{3+}$ .

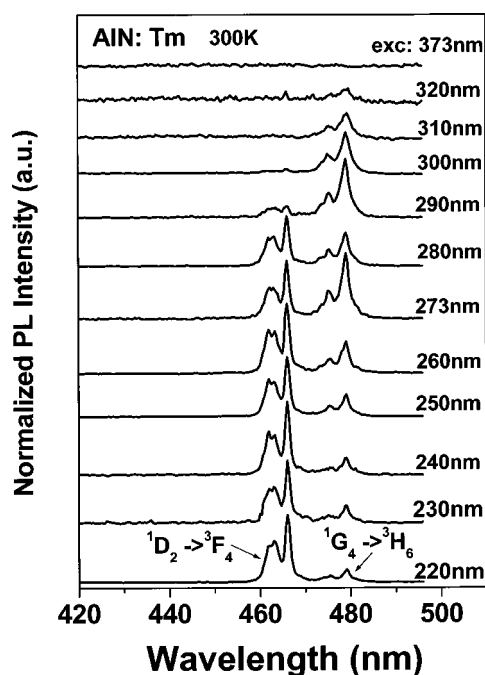


FIG. 4. Below-gap pumping of AlN:Tm using different excitation wavelengths in the UV region. The blue PL from  $\text{Tm}^{3+}$  can be excited of a wide range of wavelengths from  $\sim 320$  down to  $220$  nm (lower wavelength limit of OPO laser system).

lifetimes also provide further support that the two blue PL lines arise from different transitions of  $\text{Tm}^{3+}$ , namely,  $^1\text{D}_2 \rightarrow ^3\text{F}_4$  (465 nm) and  $^1\text{G}_4 \rightarrow ^3\text{H}_6$  (478 nm). Besides the dominant blue PL, AlN:Tm exhibited several weaker PL lines ranging from the UV to the near-infrared spectral region. Emission at  $1440$  nm was also observed from AlN:Tm (inset of Fig. 2), which arises from the well-known  $\text{Tm}^{3+}$  transition  $^3\text{H}_4 \rightarrow ^3\text{F}_4$ .<sup>17</sup> The identification of the remaining PL lines was facilitated by a careful analysis of PL lifetimes. It was found that the  $\text{Tm}^{3+}$  PL originates from four excited states of  $\text{Tm}^{3+}$ , namely, the  $^1\text{I}_6$ ,  $^1\text{D}_2$ ,  $^1\text{G}_4$ , and  $^3\text{H}_4$  with room-temperature lifetimes of  $\sim 0.5$ ,  $\sim 2$ ,  $\sim 33$ , and  $\sim 35$   $\mu\text{s}$ , respectively (Fig. 3). Since the  $^1\text{G}_4$  and  $^3\text{H}_4$  states have similar PL lifetimes, the origin of the  $\sim 805$  nm PL was clarified by pumping resonantly into the  $^1\text{G}_4$  and  $^3\text{F}_2$  excited state at  $\sim 478$  and  $\sim 675$  nm, respectively. Moreover, since the  $\sim 805$  nm PL can be pumped resonantly in the  $^3\text{F}_2$  excited state, it has to be due to the  $^3\text{H}_4 \rightarrow ^3\text{H}_6$  transition of  $\text{Tm}^{3+}$ . Based on the comparison to  $\text{Tm}^{3+}$ -doped insulating materials,<sup>16,17</sup> we tentatively located the  $^1\text{I}_6$  level below the  $^3\text{P}_0$  state. A final identification of the energy position of  $^1\text{I}_6$  and  $^3\text{P}_0$  levels, however, requires further investigations.

It is also interesting to note that the  $\text{Tm}^{3+}$  PL was efficiently excited below the bandgap of AlN using the  $250$  nm output from an OPO system. Since  $\text{Tm}^{3+}$  has no intra- $4f$  transition absorption line close to  $250$  nm,<sup>16</sup> the excitation of  $\text{Tm}^{3+}$  ions in AlN must occur through defects in the AlN host. A similar below-gap excitation mechanism was observed for AlN:Er.<sup>23</sup> Excitation-wavelength-dependent studies showed that the  $\text{Tm}^{3+}$  PL can be excited over a wide wavelength range starting from  $\sim 320$  down to  $220$  nm, as shown in Fig. 4. It can be seen that the ratio of emission from

the  $^1\text{D}_2$  ( $\sim 465$  nm) and  $^1\text{G}_4$  ( $\sim 478$  nm) levels varied as a function of excitation wavelength. This result suggests the existence of different  $\text{Tm}^{3+}$  centers, which are selectively excited through different defects.

In summary, the PL properties of  $\text{Al}_x\text{Ga}_{1-x}\text{N}:\text{Tm}$  were investigated. Under above-gap pumping, GaN:Tm exhibited only a weak blue emission from the  $^1\text{G}_4 \rightarrow ^3\text{H}_6$  transition of  $\text{Tm}^{3+}$ . A significant enhancement of the blue  $\text{Tm}^{3+}$  emission was observed from Tm-doped  $\text{Al}_x\text{Ga}_{1-x}\text{N}$  samples. Besides emission from the  $^1\text{G}_4 \rightarrow ^3\text{H}_6$  transition, a second blue emission line appeared around  $465$  nm, which was assigned to the  $^1\text{D}_2 \rightarrow ^3\text{F}_4$  transition of  $\text{Tm}^{3+}$ . The overall strongest blue PL emission was measured from  $\text{Al}_x\text{Ga}_{1-x}\text{N}:\text{Tm}$  with  $x=0.62$ . Strong blue emission from the  $^1\text{D}_2$  and  $^1\text{G}_4$  levels of  $\text{Tm}^{3+}$  was also observed from AlN:Tm under below-gap excitation. The large sensitivity of the blue emission from  $\text{Tm}^{3+}$  on the Al content of  $\text{Al}_x\text{Ga}_{1-x}\text{N}$  indicates the possibility to optimize the RE excitation and emission properties through careful bandgap engineering of the host.

The authors from H. U. acknowledge financial support by ARO through grant DAAD19-02-1-0316. The work at U. C. was supported by ARO grant DAAD 19-99-1-0348.

<sup>1</sup>A. J. Steckl and J. M. Zavada, Mater. Res. Bull. **24**, 33 (1999).

<sup>2</sup>A. J. Steckl, J. C. Heikenfeld, D. S. Lee, M. J. Garter, C. C. Baker, Y. Wang, and R. Jones, IEEE J. Sel. Top. Quantum Electron. **8**, 749 (2002).

<sup>3</sup>Mater. Res. Soc. Symp. Proc. **422** (1996).

<sup>4</sup>Proceedings of E-MRS Symposium Spring 2000, edited by J. Zavada, T. Gregorkiewicz, and A. J. Steckl [Mater. Sci. Eng., B **81**, (2001)].

<sup>5</sup>S. Morishima, T. Maruyama, M. Tanaka, Y. Masumoto, and K. Akimoto, Phys. Status Solidi A **76**, 113 (1999).

<sup>6</sup>J. Heikenfeld, M. Garter, D. S. Lee, R. Birkhahn, and A. J. Steckl, Appl. Phys. Lett. **75**, 1189 (1999).

<sup>7</sup>A. Steckl and R. Birkhahn, Appl. Phys. Lett. **73**, 1700 (1998).

<sup>8</sup>A. J. Steckl, M. Garter, D. S. Lee, J. Heikenfeld, and R. Birkhahn, Appl. Phys. Lett. **75**, 2184 (1999).

<sup>9</sup>D. S. Lee and A. J. Steckl, Appl. Phys. Lett. **82**, 55 (2003).

<sup>10</sup>W. M. Jadwisieniczak, H. J. Lozykowski, I. Berish, A. Bensaoula, and I. G. Brown, J. Appl. Phys. **89**, 4384 (2001).

<sup>11</sup>K. Gurumurugan, H. Chen, G. R. Harp, W. M. Jadwisieniczak, and H. J. Lozykowski, Appl. Phys. Lett. **74**, 3008 (1999).

<sup>12</sup>V. I. Dimitrova, P. G. Van Patten, H. H. Richardson, and M. E. Kordesh, Appl. Phys. Lett. **77**, 478 (2000).

<sup>13</sup>U. Vetter, M. F. Reid, H. Hofsaas, C. Ronning, J. Zenneck, M. Dietrich, and ISOLDE Collaboration, MRS Proceedings **743**, L6.16.1 (2003).

<sup>14</sup>D. S. Lee and A. J. Steckl, Appl. Phys. Lett. **83**, 2094 (2003).

<sup>15</sup>D. G. Ebling, L. Kirste, K. W. Benz, N. Teofilov, K. Thonke, and R. Sauer, J. Cryst. Growth **227–228**, 453 (2001).

<sup>16</sup>G. H. Dieke, Spectra and Energy Levels of Rare Earth Ions in Crystals (Wiley, New York, 1968).

<sup>17</sup>M. D. Seltzer, J. B. Gruber, M. E. Hills, G. J. Quarles, and C. A. Morrison, J. Appl. Phys. **74**, 2821 (1993).

<sup>18</sup>H. Bang, S. Morishima, Z. Li, K. Akimoto, M. Nomura, and E. Yagi, Phys. Status Solidi B **228**, 319 (2001).

<sup>19</sup>K. Takahei, A. Taguchi, H. Nakagome, K. Uwai, and P. S. Whitney, J. Appl. Phys. **66**, 4941 (1989).

<sup>20</sup>E. E. Nyein, U. Hommerich, J. Heikenfeld, D. S. Lee, A. J. Steckl, and J. M. Zavada, Appl. Phys. Lett. **82**, 1655 (2003).

<sup>21</sup>S. Kim, S. J. Rhee, X. Li, J. J. Coleman, S. G. Bishop, and P. B. Klein, J. Electron. Mater. **27**, 246 (1998).

<sup>22</sup>T. Zhang, J. Sun, N. V. Edwards, D. E. Moxey, R. M. Kolbas, and P. J. Caldwell, Mater. Res. Soc. Symp. Proc. **301**, 257 (1993).

<sup>23</sup>X. Wu, U. Hömmrich, J. D. Mackenzie, C. R. Abernathy, S. J. Pearton, R. N. Schwartz, R. G. Wilson, and J. M. Zavada, Appl. Phys. Lett. **70**, 2126 (1997).